EXPERIMENTAL STUDIES AND COMPUTER SIMULATIONS OF MAGNETOPLASTIC EFFECT

Vladimir I. Alshits[1,2], Elena V. Darinskaya[1], Marina V. Koldaeva[1],
Romuald K. Kotowski[2], Elena A. Petrzhik[1], Piotr K. Tronczyk[2]

[1]*Shubnikov Institute of Crystallography RAS, Moscow, Russia*
[2]*Department of Applied Informatics*
Polish-Japanese Academy of Information Technology, Warsaw, Poland

E-mail: rkotow@pjwstk.edu.pl

Abstract: The new relations in kinematics of the magnetoplasticity phenomenon based on the experimental studies and the computer simulations are presented. The movement of the crystal dislocation line through a random distribution of the point defects, being the obstacles for the motion of the dislocation, is discussed. It is shown that the mean value of the obstacles on the dislocation line does not depend on their concentration C in the sample and the critical dispatching force is proportional to $\sqrt{C}$.

Key words: magnetoplasticity, smart materials, computer simulations, dislocations, point defects in crystals

Introduction

The MagnetoPlastic Effect in nonmagnetic materials (MPE), was discovered in 1987 [1]. Fig. 1 shows the experimental scheme and the results obtained. The sample of the nonmagnetic material (e.g., $NaCl$, Al or ZnS) was exposed to the action of the magnetic field and after the chemical treatment the unexpected translation of the dislocations, the linear defects of the crystal lattice, was observed: the dislocations $(1, 2, 3, 4, \dots)$ moved to the new positions $(1', 2', 3', 4', \dots)$.
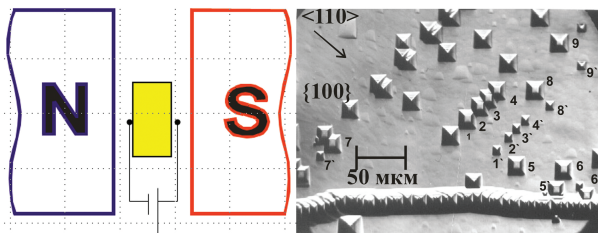

Fig. 1: Experimental scheme: crystal exposed to a static magnetic field B and the observation of the new positions of the dislocations.

The physics of the reaction of the solid to the magnetic field

It is well known that some physical processes in solids only allow for selected spin configurations. The interactions of spins with the magnetic field, having a very low energy, even mostly neglected from the energetic point of view, have a strong impact on the results of the chemical reactions, luminosity, electric conductivity, photosynthesis, etc. In our case the key phenomenon is the interaction of the dislocation with the spins of the obstacles, which in most cases are the specific point defects of the crystal lattice. Under the action of the magnetic field the reorganization of the obstacle's spin occurs, the pinning force dislocation-point defect is reduced and the dislocation can continue its motion.

There are also other conditions to be fulfilled. Particularly the depinning time τ_{dp} should be smaller than the spin-lattice relaxation time τ_{s-l}. In the opposite case the thermal chaotic vibrations practically exclude the MPE. It was observed that time τ_{dp} increases when the value of the magnetic field decreases. It means that there exists a certain B_{th} threshold value of the magnetic field B when MPE stops existing. It can be estimated from the condition $\tau_{dp}(B_{th}) \sim \tau_{s-l}$. In paper [2] such threshold values of the magnetic field in Al, $NaCl$, and LiF crystals were observed and measured. The dependence of B_{th} on the temperature was also confirmed.

Experiments [1] and [3] show that the mean route l and the density ρ_m of the mobile dislocations increase with the increasing of the $B^2 t$ value and is relatively well described by the equations

$$\Delta l \equiv l - l_0 \approx k B^2 t \,, \Delta \rho_m \equiv \rho_m - \rho_0$$
$$\approx \Delta \rho_\infty [1 - \exp(-\lambda B^2 t)] \,, \tag{1}$$

where l_0 and ρ_0 are connected with the chemical treatment of the sample crystal, $\Delta \rho_\infty = (\rho_m - \rho_0)_{B^2 t \to \infty}$, and k and λ are the constant parameters connected with a given crystal.
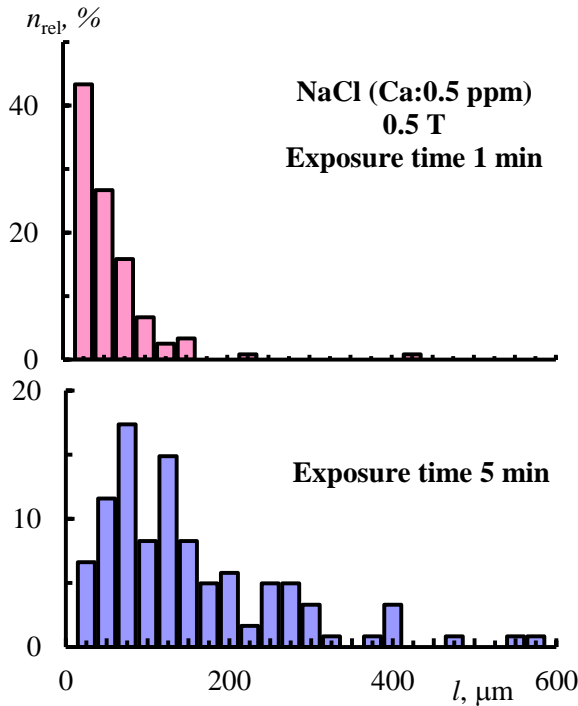
Fig. 2: Histograms for paths of dislocations in $NaCl$ crystals after 1 min and 5 min exposure times in H field of 0.5T.
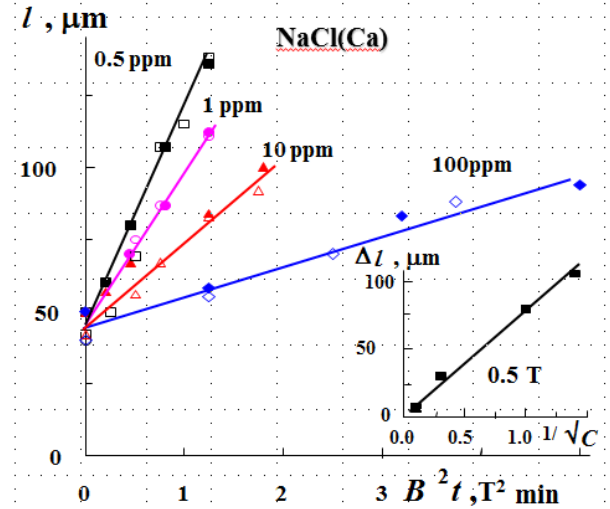

Fig. 3: Experimental results of the dependence of the mean route l of the mobile dislocations on B^2t for $NaCl$ crystals with different concentration C of the interstitial atoms Ca.

The obtained results are shown in Fig. 2 and described by Eqn. (2).

$$l = l_0 + k\frac{B^2t}{\sqrt{C}} \qquad (2)$$

Physical mechanism of MPE kinematics

It was established that motions of the mobile dislocations have a relay character. One of the arguments obtained from the experiments is that the density of mobile dislocations increases with the time of the exposition of the crystal sample to the magnetic field. The dislocations assemble to create the fields of intrinsic stresses and the mobile dislocation moves to places with the smaller stresses. Such a mechanism produces a new intrinsic stress field, and the other dislocation may follow the first one. It is obvious that for this type of motion the mean time t_m of the motion of the separate dislocations should be considerably smaller than the time t of the exposition in the magnetic field. It was found [3] that $t_m \approx 0.07t$.
It was shown [3] that in the crystals $NaCl(Ca)$ with the calcium concentration $C = 0.5$ ppm and correspondingly $C_V \sim 10^{17}$ cm^{-3}, the distance Δy between the rows of obstacles (see Fig. 3) can be approximated by

$$\Delta y \sim \frac{1}{\sqrt{2\,b\,C_V}} \sim 0.3\mu m\,. \qquad (3)$$

To cover such a distance the dislocation needs time $\Delta t \sim 0.07$s. Thetime is too big to be connected with the spin evolution time in the obstacle-dislocation line system limited by time τ_{dp} of the magnetic depinning. Because of the condition $\tau_{dp} \ll \tau_{s-l}$ and from the experiments) We have that $\tau_{s-l} \sim 10^{-4} \div 10^{-3}$s. It occurs that time τ_{dp} cannot be greater than 10^{-4}s. The next argument is that the spin transformation of obstacles on the dislocation line cannot take place simultaneously but rather step by step. The new dislocations are introduced by the weak hit on the sample just before the measurements, and they find their new stable positions according to the relief (distribution) of the long range internal stress field σ_i. The sliding force

$$F_i = b\,\sigma_i\,, \qquad (4)$$

where b – Burgers vector, is compensated by the pinning force of the point obstacles. Parallel to the growing concentration C of the point obstacles in the sample the number n_{tot} of the obstacles on the dislocation line also grows and the pinning force grows too. Consequently, the condition

$$\sigma_i \sim n_{tot}\,, \qquad (5)$$

should be fulfilled independently on the concentration C too.

We assume, in order to describe the interaction of these two forces, the approximation of the linear tension. In the case when the dislocation line has a form of an arc of a circle with a radius R spanned between the two pinning centers we have

$$R = \frac{T}{F_i}\,, \quad \text{where} \quad T \sim \frac{Gb^2}{2\pi}\,, \qquad (6)$$

and G – is the shear elastic constant of a crystal. It is seen that $G/\sigma_i \sim 10^5$ and the mean length of dislocation line in

our experiments $\bar{x} \sim 1\mu m$, so the radius of curvature R is very big, and the curvature of the dislocation line is small.

Computer Modelling of MPE

The motion of the dislocation line through the random distribution of point defects, i.e., the pinning centers, is modelled as the displacement of the geometrical line in 2D space (gliding plane) [4]. In our computer experiments the number of point defects in the modelling plane of the diameter of some tens of microns, corresponding to the field of microscope vision, was in the range from 500 to 2500.

In the computer simulations of the MPE the straight dislocation line goes from the bottom of the modelling plane until it meets the first obstacle. At that moment the two additional points outside the observation window (see Fig. 4), one to the left and one to the right, are added to the dislocation line which starts to bow creating two arcs of two curvature radii R_i, $i = 1, 2$. In the situation one of the arcs reaches the next obstacle; it divides into two new arcs.
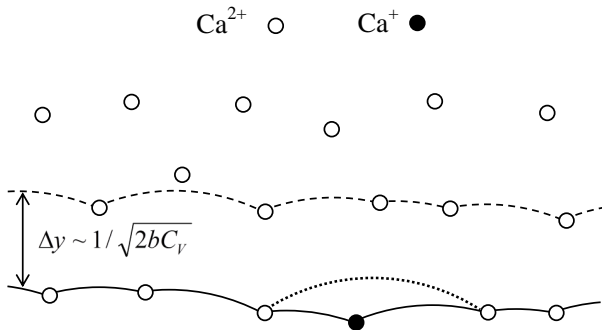
Fig. 4: Rows of obstacles in the crystal lattice.

The detachment of the dislocation arcs from the obstacle takes place when the angle α_n is smaller than the critical angle α_c (see Fig. 5). The next calculations take place without that point and the process stops when all the stop points are crossed over, and all the arcs reach their minimal radius $R = 1/F$, and there are no angles α_n smaller the critical angle α_c. It is the starting position of the computer simulation.

The algorithm of the switching on the magnetic field consists in increasing the critical angle α_c by the value $\Delta\alpha_c$. In calculations the other critical angle was used, and namely $\theta_c = \frac{1}{2}(180° - \alpha_c)$, which in the magnetic field decreased its value according to the equation

$$\theta_c^m = \theta_c - \frac{\Delta\alpha_c}{2}. \tag{7}$$

The computer experiments θ_c^m used in the following limits

$$\theta_c^m = (0.2 \div 0.3)\theta_c, \tag{8}$$

which corresponds to following values of $\Delta\alpha_c$

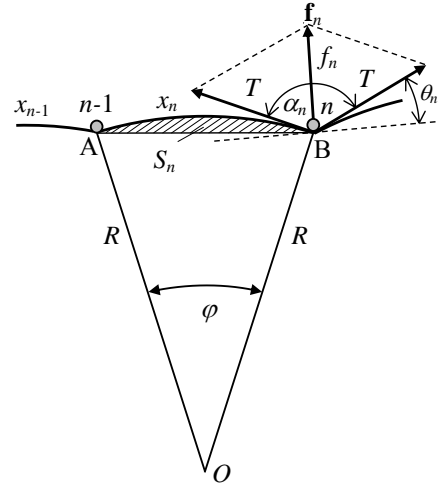Fig. 5: The angle α_n between the dislocation arcs at the obstacle n.

$$\Delta\alpha_c = 2\theta_c(0.7 \div 0.8). \tag{9}$$

After the magnetic field is switched on a certain part of obstacles on the dislocation lines with the angles θ_n in the limits $\theta_c^m < \theta_n < \theta_c$ leave the equilibrium positions, and their detachment from the obstacles occur. We call them the active obstacles. The results of the computer simulation of the dislocation displacement independence of the applied force F and the number of obstacles is shown in Fig. 6.
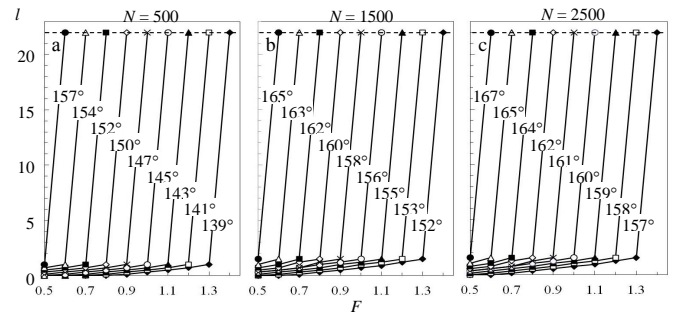
Fig. 6: Dependence of dislocation displacement on the applied force F, different values of the critical angle α_c and different number of obstacles.

In Fig. 7, an example of the normalized histograms of the discrete distrubution of the angles θ_n is given by Eqn. (10) for $N = 1500$.
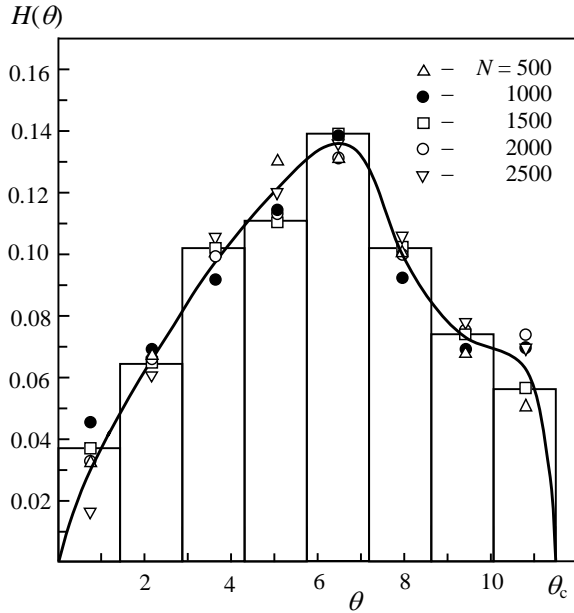
$$\Delta n(\theta_i) = n_{tot} H(\theta_i) \Delta\theta, \tag{10}$$

where

$$\int_0^{\theta_c} H(\theta)d\theta = 1. \tag{11}$$

is shown.

The scope $0 < \theta < \theta_c$ of the changes of the angle θ is divided into 8 parts of the width $\Delta\theta = \theta_c/8$. The data

Fig. 7: Normalized histograms of the distribution $H(\theta_n)$.

Table 1: Data for $\alpha_c = 157°$ and for different numbers of obstacles N

N	500	1000	1500	2000	2500
$F_i = 1/R$	0.50	0.80	0.95	1.1	1.3
n_{tot}	21	31	37	43	48
$\bar{\theta}$	10.03	10.10	10.03	10.04	10.04
$\gamma = \bar{\theta}/\theta_c$	0.873	0.878	0.873	0.873	0.873

calculated in the computer simulations and used in construction Fig. 7 are shown in Table 1.

Conclusions

In this paper the kinematical aspects of the magnetoplasticity were discussed. The connection of real experiments with the computer simulations was shown to be very fruitful. We can state that the proposed kinematical scheme successfully explains all observations made on the $NaCl$ crystals. As discussed the transformation of the structure of the point defects in the magnetic field can influence not only the mechanical but also other physical properties of the crystals, as occurs in the dielectric properties of the segnetoelectrics. It can be concluded that our research is strongly connected with the research on the smart materials.

Literature

[1] Alshits, V. I., Darinskaya, E. V., Perekalina, T. M., Urusovskaya, A. A. On the dislocation movement in NaCl crystals under a static magnetic field. *Phys. Solid States (Russ.)*, 29:467–470, 1987.

[2] Alshits V. I, Darinskaya E. V., Kazakova O. L., Mikhina E. Yu., Petrzhik E. A. Magnetoplastic effect and spin-lattice relaxation in a dislocation-paramagnetic-center system. *JETP Letters*, 63:668–673, 1996.

[3] Alshits V. I., Darinskaya E. V., Koldaeva M. V., Petrzhik E. A. *Dislocations in Solids.*, chapter Magnetoplastic Effect in Nonmagnetic Crystals, 14:333, Hirth E., J. (Ed.), Elsevier, 2008.

[4] Kotowski R., Alshits V. I., Tronczyk P. Computer Simulation of Magnetoplasticity – Movement of the Dislocation in the Magnetic Field (in Polish), *Electrical Review*, 82:80–82, 2006.